# Preparation and optical characterization of $Cu_2ZnGeSe_4$ thin films

S. Levcenko[1], R Caballero[2], L. Dermenji[3]*, E.V. Telesh[4], I.A. Victorov[4], J. M. Merino[2], E. Arushanov[3], M. Leon[2], I.V. Bodnar[4]

[1]*Helmholtz Zentrum Berlin fur Materialien and Energie GmbH, Hahn-Meitner-Platz 1, D-14109 Berlin, Germany;*
[2]*Universidad Autonoma de Madrid, Departamento Fısica Aplicada, C-XII, 28049 Madrid, Spain*
[3]*Institute of Applied Physics, Academy of Sciences of Moldova, Academiei Str. 5, MD-2028 Chişinău, Moldova*
[4]*Department of Chemistry, Belarusian State University of Informatics and Radioelectronics, Minsk, Belarus*

*E-mail: clente@list.ru Tel. (+373) 22 738170

**Abstract**

$Cu_2ZnGeSe_4$ (CZGSe) films have been fabricated by ion beam sputtering onto glass substrates at a substrate temperature of 300 and 420 K. CZGSe films were characterized by X-ray diffraction (XRD), energy dispersive X-ray spectroscopy, scanning electron microscopy and by the method of normal incidence transmittance and reflectance. XRD studies reveal an improved crystallinity of the polycrystalline CZGSe films with tetragonal structure when the substrate temperature was increased. The refraction index and extinction coefficient were extracted from the optical measurements. Spectral dependence of absorption coefficient and the energy band gaps values of CZGSe films were also determined.

**Keyword**: inorganic compounds, thin films, optical properties

## 1. Introduction

$Cu_2ZnGeSe_4$ (CZGSe) quaternary compound is considered to be a potential absorber material for photovoltaic applications [1-4]. In addition, the material in nanostructured form shows very promising thermoelectric properties with a figure of merit up to 0.55 at 450 °C [5]. However, not much information on the physical properties of CZGSe is available in comparison to close related $Cu_2ZnSnS_4$ (CZTS) and $Cu_2ZnSnSe_4$ (CZTSe) quaternary kesterite compounds. Only few experimental works on the structural [6-9], optical [1, 10-15] and electrical properties [16] of CZGSe films [10, 11] and bulk [1, 12-16] by using various techniques, such as absorption [1, 12] ellipsometry [14], Raman [15], transport [16] and far infrared spectroscopy [13] have been reported. The band-gap energy value of 1.29-1.65 eV for CZGSe [1, 10-12, 14] is in the optimum range for a single junction solar cell [17]. Several first-principles studies [2, 18-21] have been performed to investigate the phase stability and electronic structure of these materials.

The most important point defects and defect complexes have been explored and intrinsic defect formation energies were determined [21].

To further extend our knowledge on CZGSe material we performed a structural and optical characterization of CZGSe films prepared by ion beam sputtering, by using CZGSe bulk crystals as a source. By using this fabrication technique, thin film with a better semiconductor quality can be obtained in comparison to solution or spray based methods, which have low deposition rate and introduce additional impurities and defects in the grown film [22, 23]. Deposition from solution has disadvantages due to difficulty of stoichiometry and thickness control, ecological problems. Spray pyrolysis has non-uniformity of film with large grain size due to uncontrollable spray droplet and wastage of solution and film's porosity [24, 25]. The normal incidence transmittance and reflectance measurements were employed to study CZGSe optical properties in the wavelength range from 300 to 2000 nm. The values of the energy gap as well as the spectral dependence of the absorption coefficient and refraction index were derived.

## 2. Experimental details

CZGSe thin films were prepared by ion beam sputtering using CZGSe bulk crystals as target sources. The crystals were grown by the one-temperature method. Copper, zinc, germanium and selenium with a purity of > 99.999 at. % were used as starting materials. Elemental components taken in stoichiometric compositions were loaded into a double quartz ampoule, evacuated down to $10^{-3}$ Pa and placed in a furnace. The temperature was risen at ~50 K/h up to 1000-1020 K. After the isothermal exposure for 2 h, the temperature was risen up to 1200 K and maintained there for 2 h. Directional crystallization of the melt was carried out by decreasing the temperature of the furnace at ~2 K/h down to ~1020 K. Finally, a homogenizing annealing of the obtained ingots was carried out at this temperature for 300 h. Then the furnace was switched off.

The diameter of CZGSe crystals was relatively small (18 mm). This was the reason why focused argon ion beam was used during the films deposition process. We used Hall type ion source with anode layer, which has the next advantages over diode and magnetron sputtering i) high ($10^{-2}$ Pa) working vacuum ii) spatial division of areas of plasma generation and condensation iii) the minimum influence secondary electrons on substrates and, hence, the reduced heatings and degrees of radiating damages iv) absence of a high voltage on a target v) design simplicity.

Vacuum chamber was evacuated with the diffusion pump to a residual pressure of $2.7 \cdot 10^{-3}$ Pa. The working pressure was $6.7 \cdot 10^{-2}$ Pa, accelerating anode voltage – 3 kV, target current- 45

mA. The target-substrate distance was of - 80 mm and the deposition target-rate was about 0.58 nm/s. Thin films from two different deposition processes are investigated here. The main difference between both processes is the substrate temperature: room temperature and 420 K.

The composition of the crystals and thin films was determined by Energy Dispersive X-ray spectroscopy (EDX) (Oxford instruments, model INCAx-sight) inside a Hitachi S-3000N scanning electron microscope. EDX measurements were carried out at 25 kV operating voltage and the Cu K, Zn K, Ge K and Se L lines were used for quantification. The structure of the crystals and films were established by X-ray diffraction (XRD) and grazing incidence XRD (GIXRD) that were collected with a PANalytical X´Pert Pro MPD diffractometer using Cu $K_\alpha$ radiation and a multilayer mirror. Detector scans with incident angles of 0.25º, 2º and 4º were performed.

Scanning electron microscopy (SEM) was used to study the morphology of the $Cu_2ZnGeSe_4$/glass structure using a Philips XL30S FEG scanning electron microscope at 10 kV operating voltage.

The transmittance spectra were recorded with a Perkin Elmer Lambda 950 spectrophotometer at the temperature $T$ = 300 K. The thin film thickness was measured by a profilometer and SEM. The thickness of the thin films was approximately 500 nm.

### 3. Results and discussion

Table 1 shows the composition of the CZGSe films and CZGSe target. Some deficit of Zn is observed for the thin films in comparison to the content obtained for the crystal target. As it was observed for CZTS thin films grown by flash evaporation, the decreased Zn concentration after the sputtering can be related to its high partial pressure [26]. The Zn deficiency might be solved by an additional post annealing of the thin film in Zn atmosphere. No significant composition variations from point to point were found in both the bulk target and films. That suggests that the target and films are homogeneous.

Figure 1.a. shows the XRD spectra of the CZGSe bulk crystal. The main diffraction peaks of the kesterite structure are present. CZGSe target and films (see Figure 1.b.) crystallize into the tetragonal structure. While only a single phase is detected for the target sample, secondary phases are present in the thin films. Figure 1.c. displays the XRD pattern of the film grown at 420 K, in the 2θ range 25-30º, together with the Joint Committeee on Powder Diffraction Standards (JCPDS) corresponding to different phases. Two important features can be observed here: (1) there is a significant shift of the 112 diffraction peak towards higher 2θ for the lower grazing incidence angle of 0.25º and (2) the broadening of the 112 diffraction peak may be associated with presence of the secondary phases such as Cu-Se, ZnSe and $Cu_2GeSe_3$, especially

on the surface. A similar behavior has been observed by Uday Bahaskar et al. [11]. They observed the presence of $Cu_{2-x}Se$, ZnSe and $Cu_2GeSe_3$ for CZGSe samples grown at 523 K prepared by co-evaporation. Although a homogeneous composition has been obtained by EDX measurements, the GIXRD patterns reveal the non-uniform distribution of the elements through the layer as shown in Figure 1.c. In other words, the EDX results reveal the lateral homogeneity but the GIXRD results indicate the vertical inhomogeneity of the CZGeS films composition. As expected, the increased substrate temperature led to an enhanced crystallinity of the films. This enhanced crystalline quality for the sample grown at 420 K is also observed by SEM cross-section pictures (see Figure 2). Larger grain sizes and a columnar structure are formed for the sample deposited at higher temperature.

The optical transmission (*T*) and reflectivity (*R*) at near normal incidence of the CZGSe films prepared at $T_{sub}$ = 300 and 420 K are plotted in Figs. 3(a) and 3(b). To obtain the CZGSe optical constants from *T* and *R* measurements a three layer model (air, thin absorbing film and non-absorbing glass substrate) has been considered [27]. Note that, the XRD data did not show any preferential orientation of the secondary phases in the grown films, so that our approach to model absorber layer as a one layer can be considered as a good approximation, even if some secondary phases inclusions present in the film. The employed model allows the formulation of analytical expressions for the optical transmittance *T*(*n*, k, *d*, *s*) and reflectance *R*(*n*, k, *d*, *s*) in terms of the refractive index and extinction coefficient of the thin film, *n(λ)* and *k(λ)*, the film thickness *d*, the refractive index of the transparent substrate *s*, and wavelength of light, $\lambda$ [28]. The theoretical expressions for *T* and *R* are given by [29, 30]

$$T = Ax/\left(B - 2Cx\cos\varphi + 2Dx\sin\varphi + Ex^2\right), \quad (1)$$

$$R = \left(A' + B'x^2 + 2C'x\cos\varphi + 4D'x\sin\varphi\right)/\left(E' + F'x^2 + 2G'x\cos\varphi + 4H'x\sin\varphi\right), \quad (2)$$

where

$$A = 16s(n^2 + k^2),$$
$$B = \left[(n+1)^2 + k^2\right]\left[(n+1)(n+s^2) + k^2\right],$$
$$C = \left[n^2 - 1 + k^2\right]\left[n^2 - s^2 + k^2\right] - 2k^2(s^2+1),$$
$$D = k\left[(n^2 - s^2 + k^2) + (s^2+1)(n^2 - 1 + k^2)\right],$$
$$E = \left[(n-1)^2 + k^2\right]\left[(n-1)(n-s^2) + k^2\right],$$
$$\varphi = 4\pi nd/\lambda,$$
$$x = \exp(-\alpha d),$$
$$A' = \left[(n-1)^2 + k^2\right]\left[(n+s)^2 + k^2\right],$$
$$B' = \left[(n-s)^2 + k^2\right]\left[(n+1)^2 + k^2\right],$$
$$C' = (n^2 + k^2)(1+s^2) - (n^2 + k^2)^2 - s^2 - 4sk^2,$$

$$D' = k(s-1)(n^2+k^2+s),$$
$$E' = \left[(n+1)^2+k^2\right]\left[(n+s)^2+k^2\right],$$
$$F' = \left[(n-1)^2+k^2\right]\left[(n-s)^2+k^2\right],$$
$$G' = (n^2+k^2)(1+s^2)-(n^2+k^2)^2-s^2+4sk^2,$$
$$H' = k(s+1)(n^2+k^2-s).$$

In order to determine *n* and *k* for each single wavelength we substituted the measured thickness *d* of the film and the value *s* = 1.45 for the s refractive index of the substrate in the equation system

$$T(n,k) - T_{\exp} \le \Delta T, \quad (3)$$

$$R(n,k) - R_{\exp} \le \Delta R, \quad (4)$$

where $T_{exp}$, $T$, $R_{exp}$, $R$,- experimental and theoretical values of transmittance and reflectance data respectively and $\Delta T$, $\Delta R$ are the spectral resolutions. A known complication [31] associated with these relations (3), (4) is the existence of (*n, k)* multiple solutions for singular values of $T_{exp}$, $R_{exp}$ and *d*. Furthermore, at some specific wavelengths *n(λ)*and *k(λ)* curves exhibit discontinuities which are typical for the method of normal incidence transmittance and reflectance [27, 31]. To restict the possibility of multiple solutions we solved the equation system (3)-(4) in the region 2.5-3.5 for *n* and in the region 0-1.5 for *k* . Although we allowed a variation of *d* by 10% of its nominal value there are some spectral regions in which solutions of the equation system (3)-(4) could not be found. To overcome this computational problem we used the empirical Sellmeier equations for *n* and *k* [32]:

$$n(\lambda) = \sqrt{A_1\lambda^2/(\lambda^2 - A_2^2)}, \quad (5)$$

$$k(\lambda) = \left[n(\lambda)B_1\lambda\right]^{-1}, \quad (6)$$

where, $A_i$(*i*=1, 2) and $B_1$ are the fitting parameters. Note that here we omitted $A_0$ in the numerator of Eq.5 and $B_2$ second and $B_3$ third order terms in the expansion of the *k(λ)*in Eq.6 as they do not influence on the goodness of our fit to $T_{exp}$ and $R_{exp}$ data. The fitting results of the Sellmeier empirical relationship to $T_{exp}$ and $R_{exp}$ data in the region of weak absorption are plotted in Fig. 3. The Sellmeier Eqs. 5-6 describe well the spectral variation of the optical transmission and reflectivity of the CZGSe thin films. The obtained fitting $A_i$ and $B_1$ parameters of Eqs. 5-6 are summarized in Table 2. It is worth noting that Eq.5 can be used for estimation of the $\varepsilon_\infty$ high-frequency dielectric constant as for limit case $\lambda \to \infty$, the electronic contribution to the dielectric function approaches the limiting value**,** i. e., $\varepsilon_\infty = n^2(\lambda \to \infty) = A_1$, which is equal to ≈ 7.2 and 7.7 for CZGSe films prepared at 300 and 420 K, respectively.

The calculated values of the *n* and *k* of the CZGSe film deposited at 420K are plotted in Fig. 4 and agree well with the values of Sellmeier empirical dispersion equations (5)-(6). For comparison purposes the ellipsometry data for CZGSe bulk poly-crystals [14] are also shown in Fig. 4. Our values of extinction coefficient *k* are found to be smaller than for polycrystals. This discrepancy in *k* might be due to uncorrected surface effects for the bulk samples [33] and\or to the different density of the crystalline grains in the film and bulk samples [27]. Although the calculated constants show some uncertainty in their values, which can especially be seen for *n*-values *(*Fig. 4), they describe experimental $T_{exp}$, $R_{exp}$ data with the same accuracy as Sellmeier model.

The spectral dependence of absorption coefficient, $= )\lambda( \alpha k()\lambda 4 \lambda/ \pi$, obtained from the Sellmeier Eq.6 and from numerical solution of Eqs. 3-4 is shown in Fig. 5. The studied samples show a significant absorption of about ~$10^3$ $cm^{-1}$ in the region >1(1.2) eV for CZGSe $T_{sub}$ = 420 (300) K, respectively. It is interesting to note that below the band gap $\alpha$ derived from Eqs. 3-4 exhibits structures, while $\alpha$ derived from Eq. 6 shows a typical gradual increase of $\alpha$ in this spectral range with the photon energy. Due to the fact that these found structures in $\alpha$ correlate well with minima/maxima of the interference fringes observed in $T_{exp}$ and $R_{exp}$ data we cannot conclude that they are related to presence of the defects/impurities absorption in the grown films. On the other hand, the used Sellmeier Eq. for $k(\lambda)$ is not valid for the case of the localized absorption bands in the region of the weak absorption, where the interference extremes are well visible [28, 30]. Further measurements on CZGSe thin films with different thickness could clarify the origin of these possible structures in $\alpha$ below the band gap. It is expected that a variation of the film thickness changes the minima/maxima of interference fringes positions, while impurities/ defects absorption band possibly present in CZGSe thin films will remain at the same spectral position independently on the thin film thickness.

We made our further analysis of high values of $\alpha$ (~$10^4$ $cm^{-1}$) under the assumption of direct-gap semiconductors:

$$\alpha E = A(E - E_g)^{1/2}, \qquad (7)$$

where $E$ is the photon energy, and $A$ is a temperature independent constant that depends on the effective mass and the refractive index. The $(\alpha E)^2$ spectra show a linear dependence with the photon energy over an appreciable energy range, revealing the existence of direct band gap in CZGSe films (Fig.6). From the extrapolation of $(\alpha E)^2$ vs $E$ curves to $(\alpha E)^2 = 0$, the value of $E_g$ has been estimated. The values are equal to 1.52 and 1.17 eV for the band gaps of CZGSe prepared at the substrate temperature of 300 and 420 K, respectively, showing a decrease of $E_g$ when increasing the substrate temperature. The possible presence of the secondary phases like

$Cu_2GeSe_3$ and $Cu_{1.8}Se$ with $E_g$ of 0.77 [34] and 1.23 eV [35], respectively, may reduce the derived band gap values for CZGeSe. Since is not clear if the sample grown at 420 K has more content of the secondary phases than one grown at 300K we do not relate the found 1.17eV band gap with the influence of the secondary phases. Here, it should be also noted that the band gap values for CZGeSe single crystals range from 1.29eV [7] to 1.63eV [1]; which is close to our results. Since is not clear yet whether the growing conditions or chemical composition influence on the CZGeSe band gap the interpretation of the discrepancy in the derived band gap value requires great care. Another reason for the variation $E_g$ might be due to disordered structure of CZGSe film by analogy with the case of the Sn-based kesterites ($Cu_2ZnSnS_4$) [36, 37]. The obtained $E_g$ values are in reasonable agreement with those reported for CZGSe films prepared by the selenization method (1.34-1.65 eV) [10] and co-evaporation technique ( 1.45-1.63 eV) [11]. Note, that a similar trend in $E_g$ decrease was observed for CZGSe films prepared by co-evaporation technique where it was found $E_g \approx 1.63$ and 1.45 eV for $T_{sub}$ = 573 and 623 K, respectively [11].

## 4. Conclusions

$Cu_2ZnGeSe_4$ thin films were prepared by ion beam sputtering at the substrate temperatures of 300 and 420 K. A significant enhanced crystallinity of the films was observed by XRD and SEM for the samples using higher substrate temperature. The crystal structure of the $Cu_2ZnGeSe_4$ crystal and thin films was found to be tetragonal. Secondary phases such as $Cu_{1.8}Se$ and $Cu_2GeSe_3$ were identified by X-ray diffraction for the thin films. The spectral dependence of refraction index, extinction and absorption coefficients as well as the energy band gaps values of CZGSe films was derived from the incidence transmittance and reflectance data analysis based on three layer model (air, thin absorbing film and non-absorbing glass substrate).

## Acknowledgments

Financial supports from IRSES PVICOKEST 269167, MICINN projects (KEST-PV; ENE2010-21541-C03-01/-02/-03) and FRCFB 13.820.05.11/BF projects are acknowledged. RC also acknowledges financial support from Spanish MINECO within the program Ramón y Cajal (RYC-2011-08521).

## References

[1] H. Matsushita, T. Maeda, A. Katsui, T. Takizawa, J. Cryst. Growth 208 (2000) 416-422.

[2] Q. Guo, G.M. Ford, W.-C. Yang, C.J. Hages, H.W. Hillhouse, R. Agrawal, Sol. Energy Mat. Sol. Cells 105 (2012) 132-136.

[3] Q. Shu, J.H. Yang, S. Chen, B. Huang, H. Xiang, X.G. Gong, S.H. Wei, Phys. Rev. B 87 (2013) 115208.

[4] K. Timmo, M. Kauk-Kuusik, M. Altosaar, J. Raudoja, T. Raadik, M. Grossberg, T. Varema, M. Pilvet, I. Leinemann, O. Volobujeva, E. Mellikov, Proceedings of the 28th European Photovoltaic Solar Energy Conference, Paris, France, Sept 30–Oct 4, 2013; EU PVSEC Proceedings (2013) 2385-2388.

[5] M. Ibáñez, R. Zamani, A. La Londe, D. Cadavid, W. Li, A. Shavel, J. Arbiol, J.R. Morante, S. Gorsse, G.J. Snyder, A. Cabo, J. Am. Chem. Soc. 134 (2012) 4060-4063.

[6] W. Schafer, R. Nitsche, Mater. Res. Bull. 9 (1974) 645-654.

[7] D. M. Schleich, A. Wold, Mater. Res. Bull. 12 (1977) 111-114.

[8] O. V. Parasyuk, L.D. Gulay, Ya. E. Romanyuk, L.V. Piskach, J. Alloys Comp. 329 (2001) 202-207.

[9] Ya. E. Romanyuk, O.V. Parasyuk, J. Alloys Comp. 348 (2003) 195-202.

[10] H. Matsushita, T. Ochiai, A. Katsui, A. Katsui, J. Cryst. Growth 275 (2005) e995-e999.

[11] P.U. Bhaskar, G.S. Babu, Y.B.K. Kumar, V.S. Raja, Thin Solid Films 534 (2013) 249-254.

[12] C. Lee, C.D. Kim, J. Korean Phys. Soc. 37 (2000) 364-367.

[13] M. Himmrich, H. Haeuseler, Spectrochim. Acta A, Mol. Spectrosc. 47 (1991) 933-942.

[14] M. León, S. Levcenko, R. Serna, A. Nateprov, G. Gurieva, J. M. Merino, S. Schorr and E. Arushanov, Mater. Chem. Phys. 141 (2013) 58-62.

[15] M. Guc, S. Levcenko, V. Izquierdo-Roca, X. Fontane, E. Arushanov and A. Pérez Rodríguez, J. Appl. Phys. 114, 193514/9 (2013).

[16] M. Guc, K.G. Lisunov, E. Hajdeu, S. Levcenko, V. Ursaki, E. Arushanov, Solar Energy Materials & Solar Cells 127 (2014) 87–91.

[17] J. Nelson, The Physics of Solar Cells, Imperial College Press, London, 2003.

[18] S. Nakamura, T. Maeda, T. Wada, Jpn. J. Appl. Phys. 49 (2010) 121203.

[19] S. Chen, X. G. Gong, A. Walsh, S-H Wei, Phys. Rev. B 79 (2009) 165211.

[20] S. Chen, A. Walsh, Y. Luo, J.H. Yang, X.G. Gong, S.H. Wei, Phys. Rev. B 82 (2010) 195203.

[21] J.M. Raulot, C. Domain, J.F. Guillemoles, J. Phys. Chem. Sol. 66 (2005) 2019-2023.

[22] Solution Processing of Inorganic Materials. ed. by D.B.Mitzi, 2009. John Wiley & Sons Inc.

[23] G.Il'chuc et al., J. Nano-Electron. Phys.,1(2009), No2, 36-42.

[24] S.M. Rozati, T. Gani, Am.J. Appl.Sci (2005),No2, 1106-1108.

[25] B.G. Jeyaprakash, R. Ashokkumar, K. Kesaran, A. Amalarani, J.of Am.Sci.,6(2010),No3, 22-26

[26] R. Caballero, V. Izquierdo-Roca, J.M. Merino, E.J. Friedrich, A. Climent-Font, E. Saucedo, A. Pérez-Rodríguez, M. León, Thin Solid Films 535 (2013) 62-66.
[27] K. Orgassa, U. Rau, H.W. Schock, J.H. Werner, Proc. 3rd World Conf. PV Energy conversion, 1 (2003) 372-375.
[28] L.L. Kazmerski, M. Hallerdt, J. Ireland, R.A. Mickelsen, W.S. Chen, J. Vac. Sci. Technol. A, 1 (1983) 395-398.
[29] H.S. Soliman, M.M. El Nahas, O. Jamjoum, K.A. Mady, J. Mater. Sci., 23 (1988) 4071-4075.
[30] R. Swanepoel, J. Phys. E, 16 (1983) 1214-1224.
[31] R.E. Denton, R.D. Campbell, S.G. Tomlin, J. Phys. D: Appl. Phys., 5 (1972) 852-864.
[32] D. Poelman, P.F. Smet, J. Phys. D: Appl. Phys., 36 (2003) 1850-1857.
[33] D. E. Aspnes, A.A. Studna, Phys. Rev. B 27 (1983) 985-1009.
[34] B.K. Sarkar, A.S. Verma, P.S. Physica B 406 (2011) 2847-2850.
[35] B.A. Mansour, I.K. El Zawawi, M. Kamal, T.A. Hameed, Journal of Ovonic Research 6 (2010) 193-200.
[36] J. S. Scragg, L. Choubrac, A. Lafond, T. Ericson, and C. Platzer-Björkman, Appl. Phys. Lett. 104 (2014) 041911.
[37] M. Grossberg, J. Krustok, J. Raudoja, T. Raadik, Appl. Phys. Lett. 101 (2012) 102102.

Figure

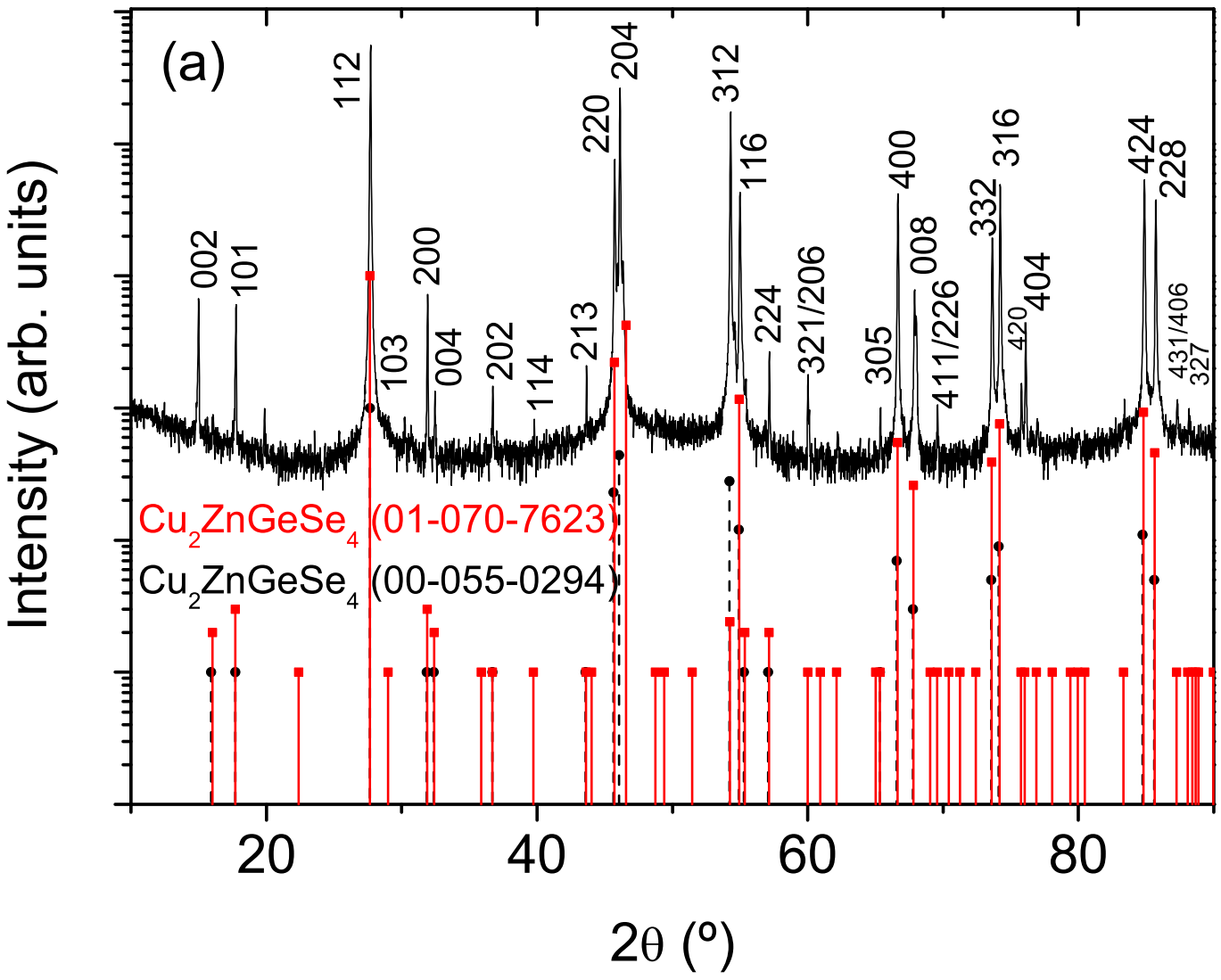
(a)
Intensity (arb. units)
2θ (°)
20
40
60
80
002
101
112
103
200
004
202
114
213
220
204
312
116
224
321/206
305
400
008
411/226
332
316
420
404
424
228
431/406
327
Cu2ZnGeSe4 (01-070-7623)
Cu2ZnGeSe4 (00-055-0294)

Figure

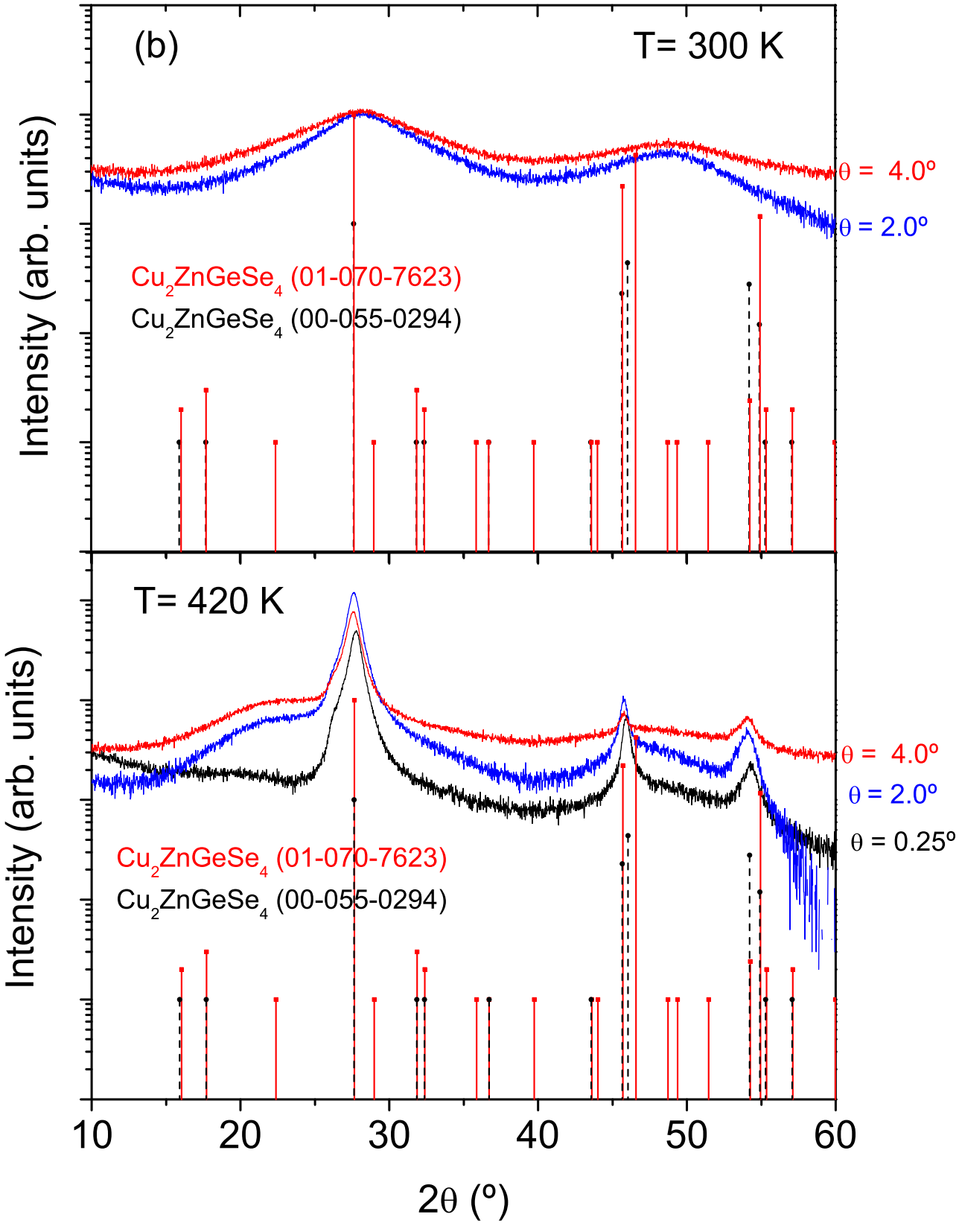
(b)
T= 300 K
Intensity (arb. units)
θ = 4.0º
θ = 2.0º
Cu2ZnGeSe4 (01-070-7623)
Cu2ZnGeSe4 (00-055-0294)
T= 420 K
Intensity (arb. units)
θ = 4.0º
θ = 2.0º
θ = 0.25º
Cu2ZnGeSe4 (01-070-7623)
Cu2ZnGeSe4 (00-055-0294)
10
20
30
40
50
60
2θ (º)

Figure

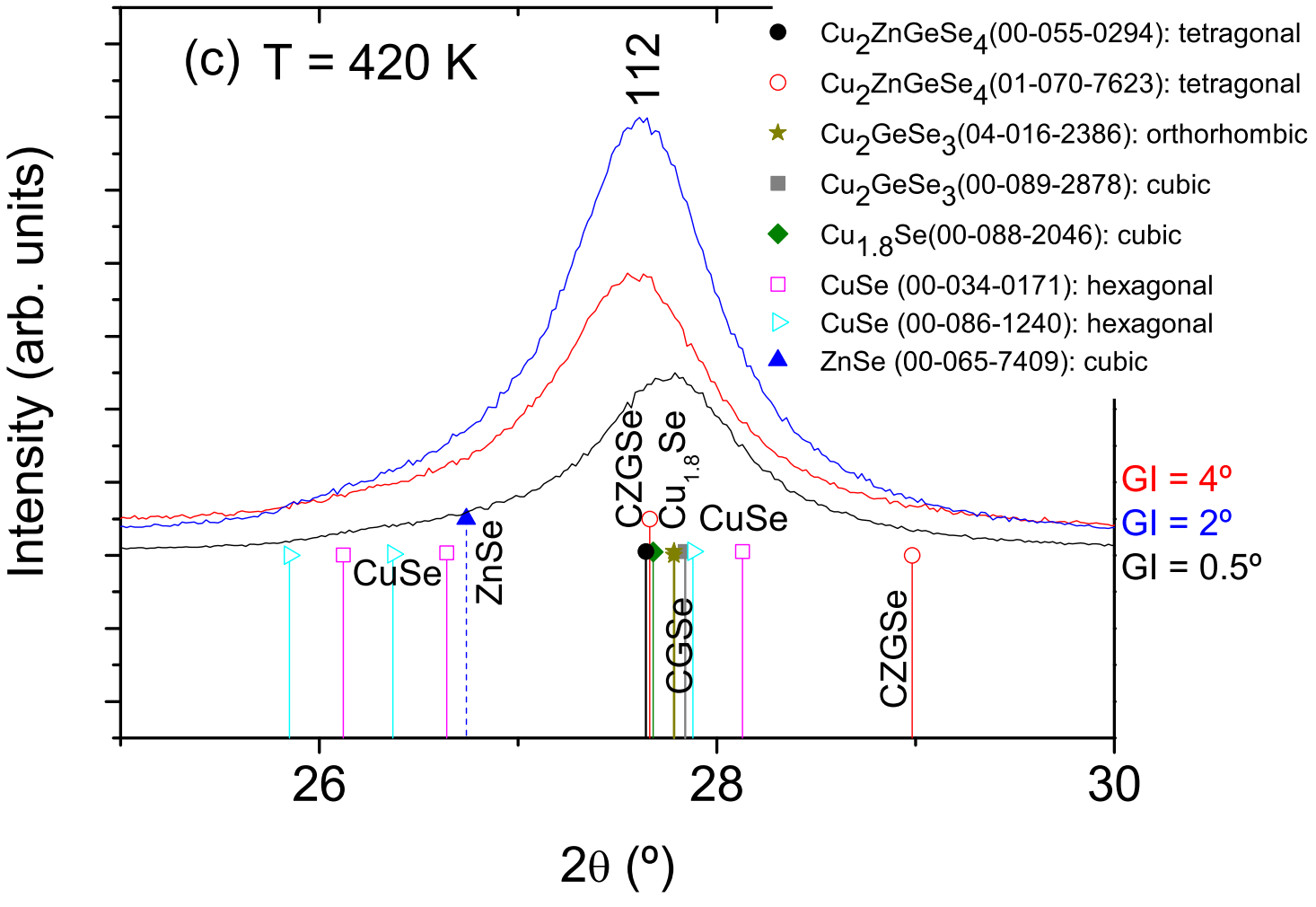
(c) T = 420 K
112
Cu2ZnGeSe4(00-055-0294): tetragonal
Cu2ZnGeSe4(01-070-7623): tetragonal
Cu2GeSe3(04-016-2386): orthorhombic
Cu2GeSe3(00-089-2878): cubic
Cu1.8Se(00-088-2046): cubic
CuSe (00-034-0171): hexagonal
CuSe (00-086-1240): hexagonal
ZnSe (00-065-7409): cubic
GI = 4º
GI = 2º
GI = 0.5º
CZGSe
Cu1.8Se
CuSe
CuSe
ZnSe
CGSe
CZGSe
Intensity (arb. units)
26
28
30
2θ (º)

Figure

Click here to download high resolution image

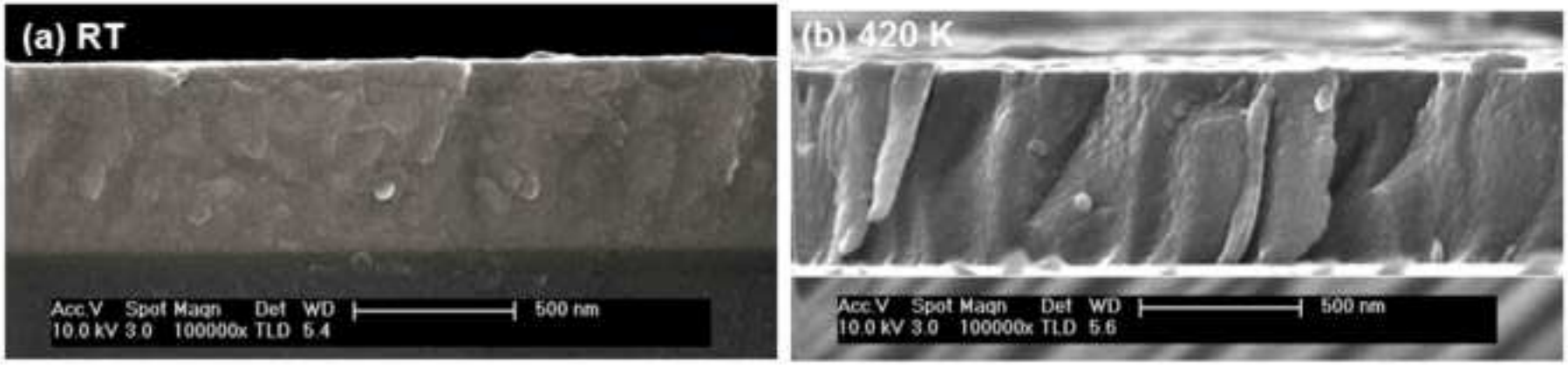

Figure

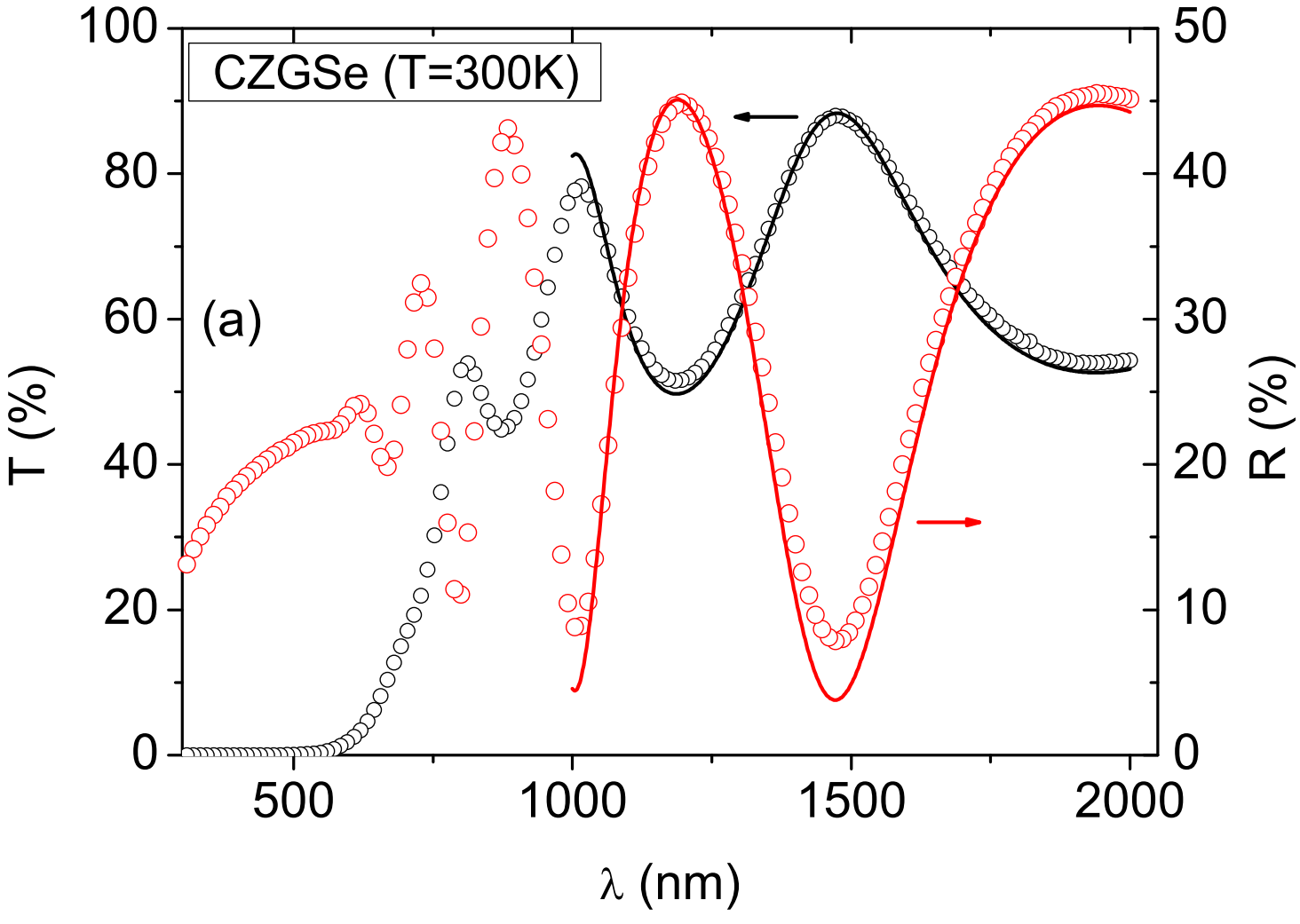
CZGSe (T=300K)
(a)
T (%)
R (%)
λ (nm)
100
80
60
40
20
0
50
40
30
20
10
0
500
1000
1500
2000

Figure

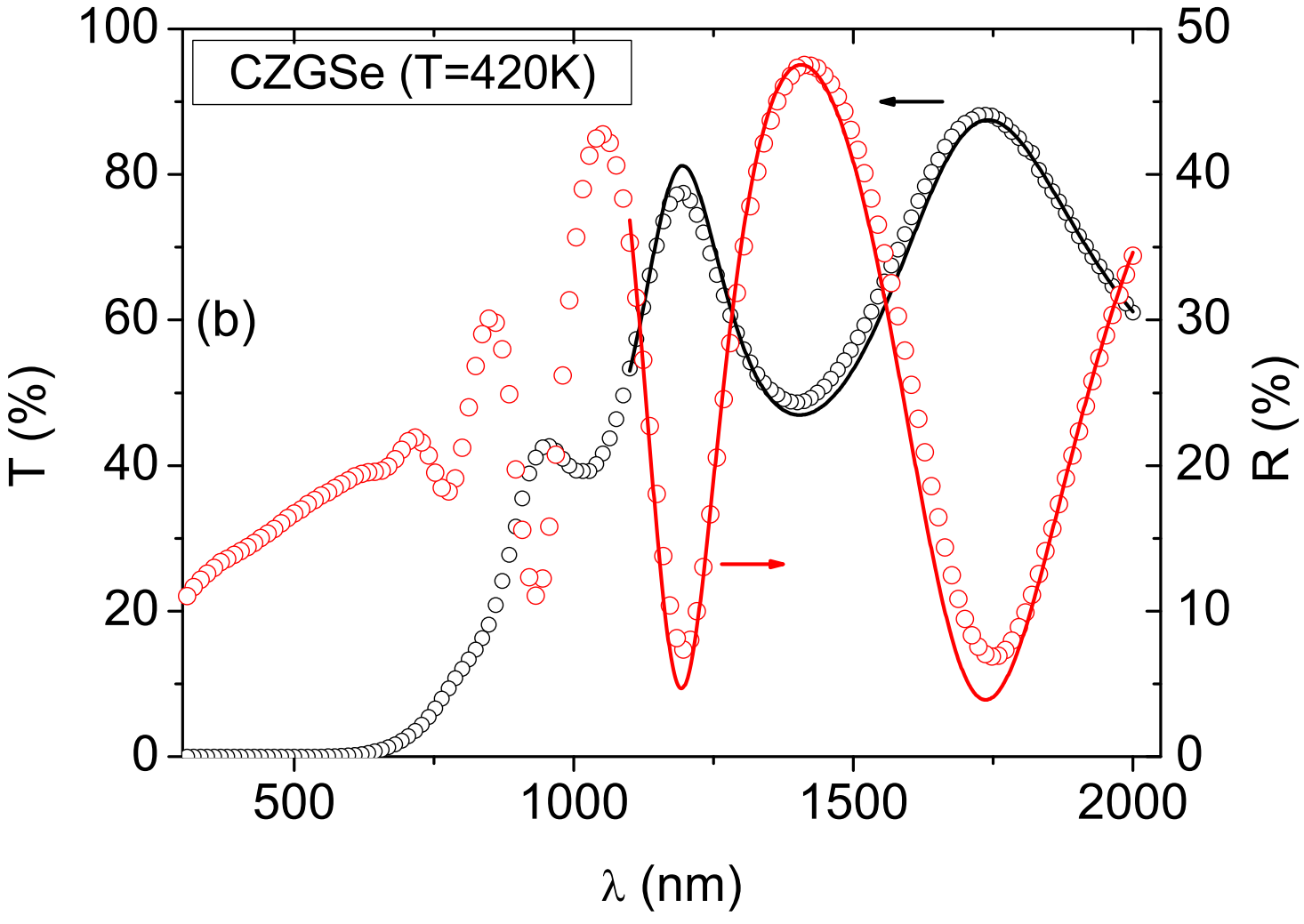
CZGSe (T=420K)
(b)
T (%)
R (%)
λ (nm)
100
80
60
40
20
0
50
40
30
20
10
0
500
1000
1500
2000

Figure

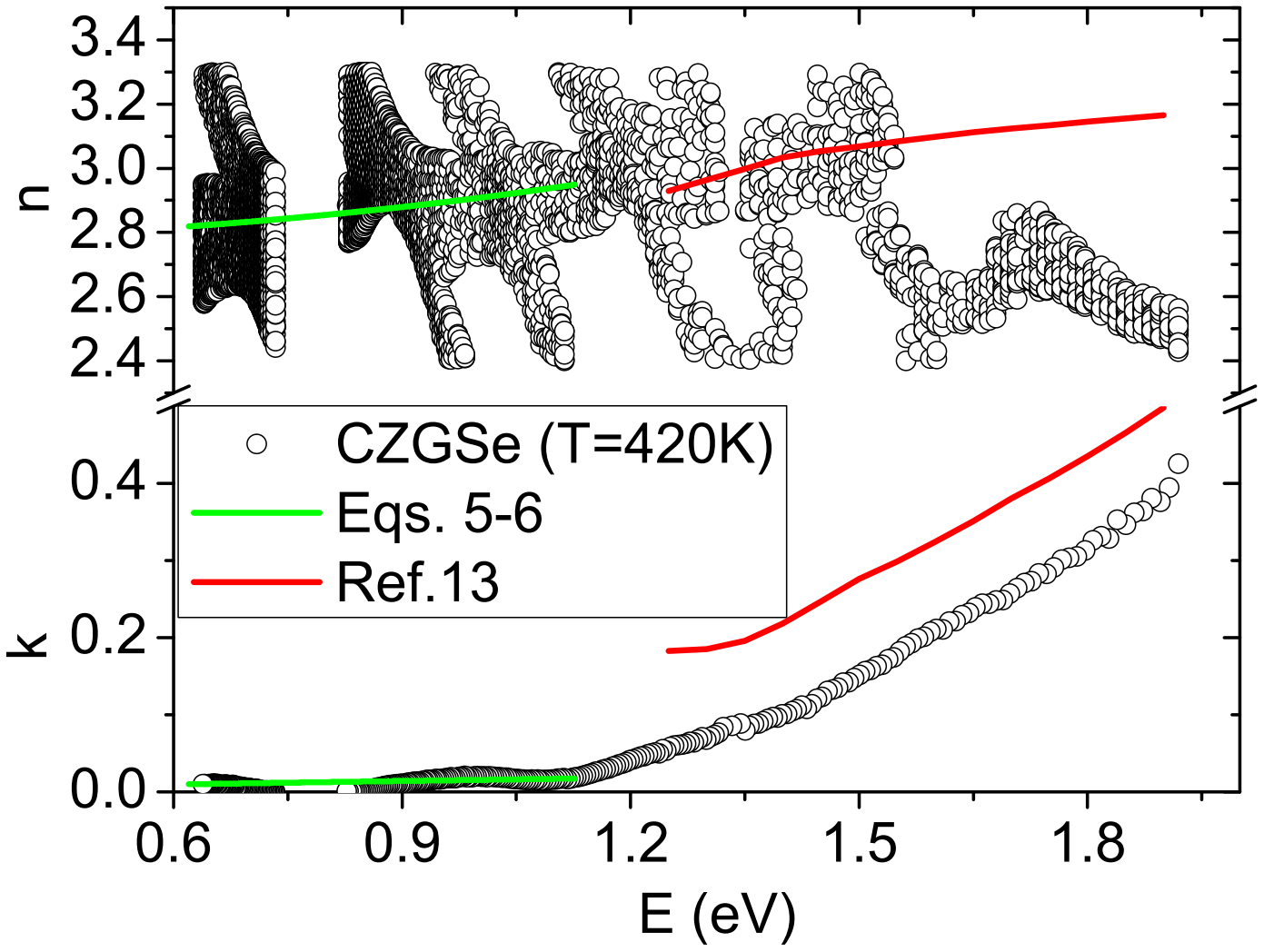
n
3.4
3.2
3.0
2.8
2.6
2.4
k
0.4
0.2
0.0
CZGSe (T=420K)
Eqs. 5-6
Ref.13
0.6
0.9
1.2
1.5
1.8
E (eV)

Figure

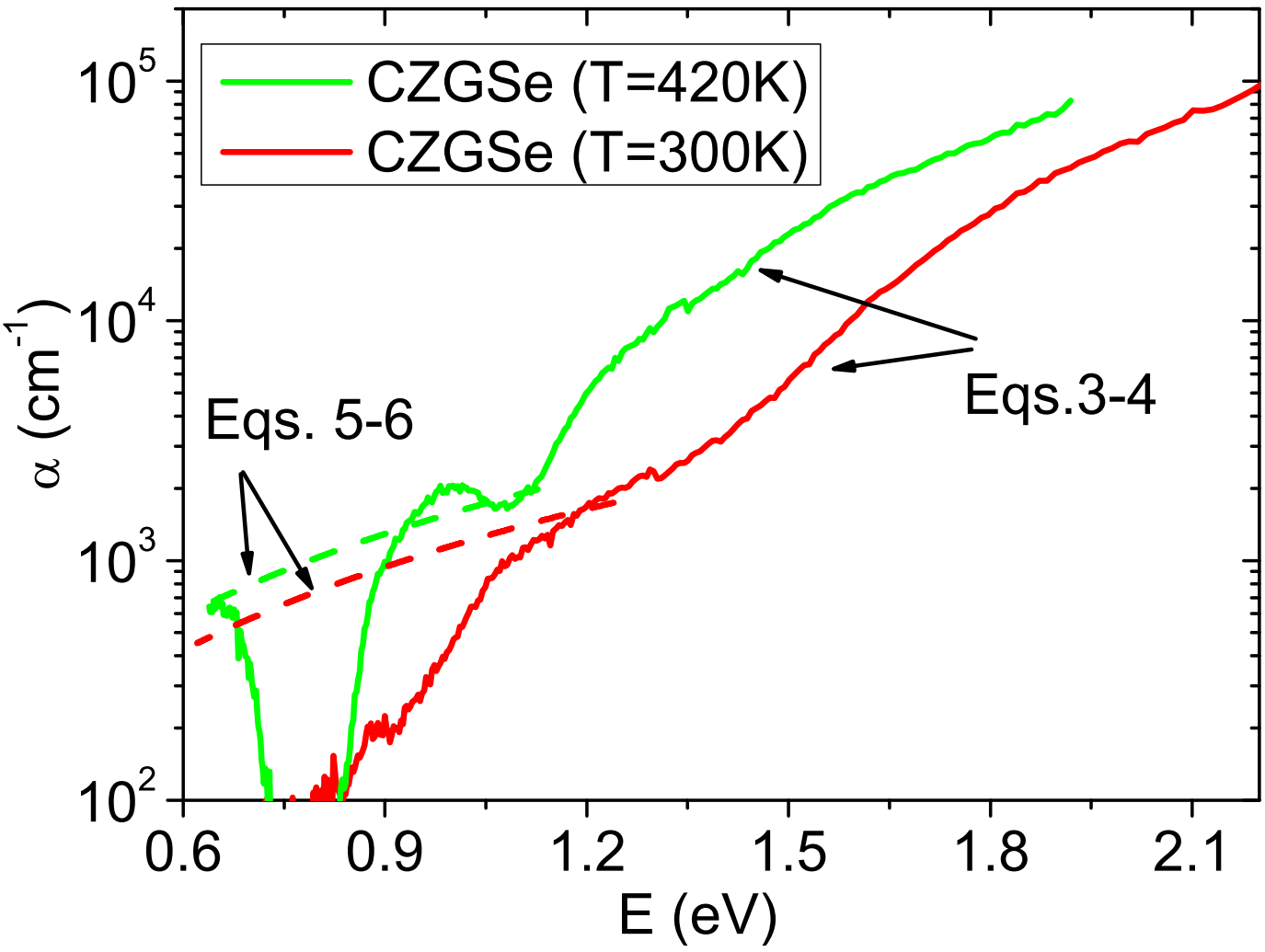
CZGSe (T=420K)
CZGSe (T=300K)
Eqs. 5-6
Eqs.3-4
α (cm-1)
E (eV)
10^5
10^4
10^3
10^2
0.6
0.9
1.2
1.5
1.8
2.1

Figure

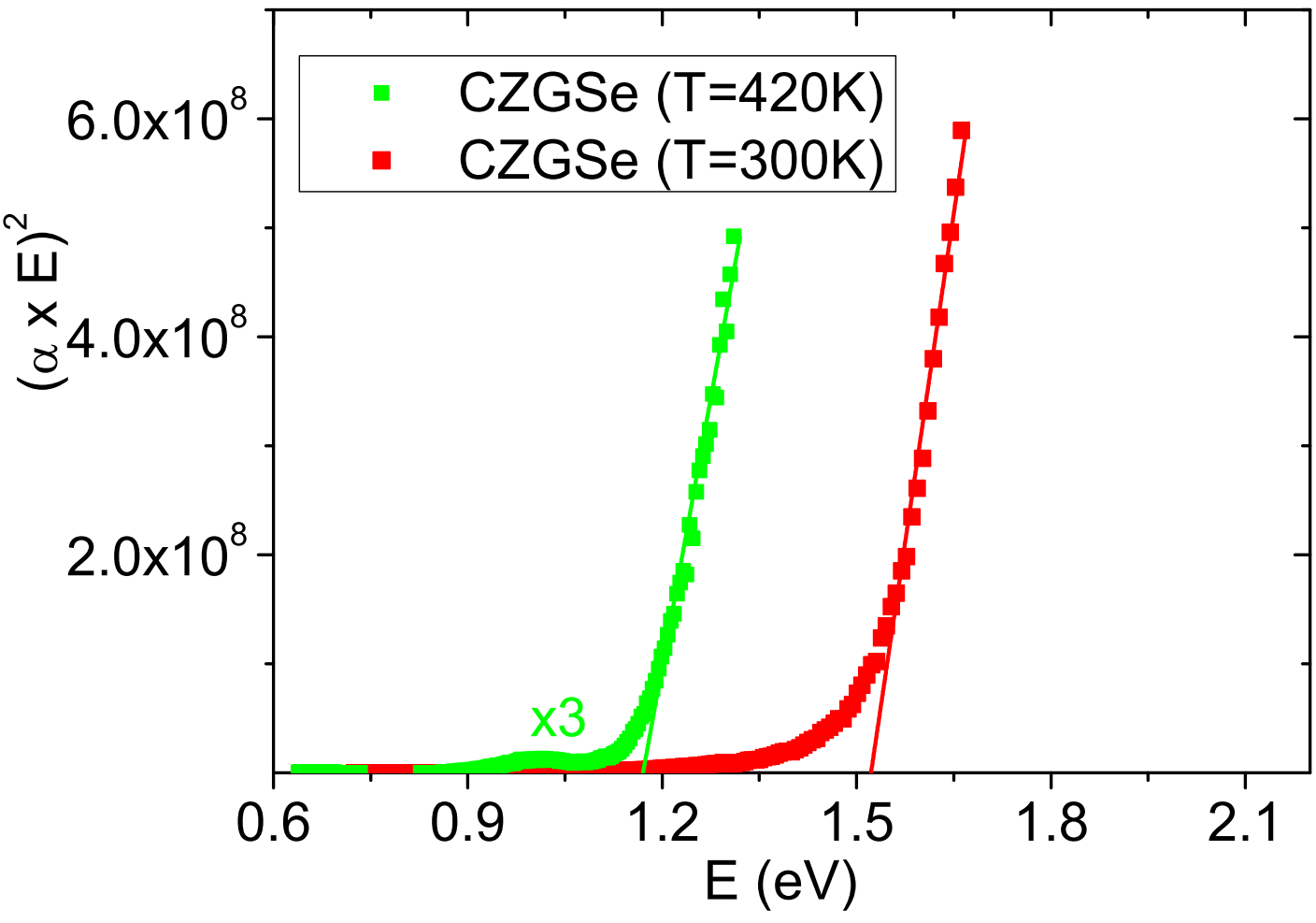
CZGSe (T=420K)
CZGSe (T=300K)
x3
$(\alpha \times E)^2$
$6.0x10^8$
$4.0x10^8$
$2.0x10^8$
0.6
0.9
1.2
1.5
1.8
2.1
E (eV)

## Figure Captions

**Fig. 1.** XRD patterns of $Cu_2ZnGeSe_4$ (a) crystal and (b) thin films. (c) 112 diffraction peak of the film grown at substrate temperature of 420 K. JCPDS files of the CZGSe and secondary phases are given as references.

**Fig. 2.** Cross sectional SEM micrographs of the $Cu_2ZnGeSe_4$ thin films grown at (a) room temperature and (b) 420 K. Operation voltage = 10 KV and magnification = 100K x have been used.

**Fig. 3.** Experimental T and R values (open circles) of $Cu_2ZnGeSe_4$ films deposited onto glass substrates at substrate temperatures $T_{sub}$ = 300 (a) and 420 K(b).Solid lines represent fits to Eqs. (1)-(2) by substituting Sellmeier Eqs. (5)-(6).

**Fig. 4.** Solution branches for refractive index $n$ and extinction coefficient $k$ of $Cu_2ZnGeSe_4$ films deposited onto glass substrates at substrate temperatures $T_{sub}$ = 420 K. Open circles reperesent numerical fits to Eqs. (1)-(2) based on the restriction Eqs. (3)-(4), the solid line in the range 0.6-1.2 eV show numerical fits by using Sellmeier Eqs. (5)-(6) and solid lines in the range 1.3-1.9 represent ellipsometry data taken from [13], respectively.

**Fig. 5.** $\alpha$ vs $E$ for $Cu_2ZnGeSe_4$ films deposited onto glass substrates at substrate temperatures $T_{sub}$ = 300 and 420 K. The solid lines represent numerical fits to Eqs.(1)-(2) based on the restriction Eqs.(3)-(4); dashed lines in the range 0.6-1.2 eV show numerical fits by using Sellmeier Eqs. (6).

**Fig. 6.** Dependence of the quantity $(\alpha E)^2$ on the photon energy $E$ for $Cu_2ZnGeSe_4$ films produced at substrate temperature $T_{sub}$ = 300 and 420 K.

**Table 1**

Composition of $Cu_2ZnGeSe_4$ bulk crystal and thin films measured by EDX.

| Compounds | Cu, at. % | Zn, at.% | Ge, at.% | Se, at.% |
|---|---|---|---|---|
| $Cu_2ZnGeSe_4$ (bulk crystal) | 26.21 | 11.30 | 13.66 | 48.83 |
| $Cu_2ZnGeSe_4$ (film, 300 K) | 23.85 | 8.80 | 12.30 | 55.05 |
| $Cu_2ZnGeSe_4$ (film, 420 K) | 27.27 | 7.50 | 13.13 | 51.94 |

**Table 2**

Values of the Sellmeier parameters (Eqs. (5)-(6)) of $Cu_2ZnGeSe_4$ thin films obtained by fitting the spectral dependence of normal incidence transmittance and reflectance data to Eqs. (1)-(2).

| Compounds | $A_1$ | $A_2$, μm | $B_1$, $\mu m^{-1}$ |
|---|---|---|---|
| $Cu_2ZnGeSe_4$ (film, 300 K) | 7.21 | 0.29 | 25.8 |
| $Cu_2ZnGeSe_4$ (film, 420 K) | 7.66 | 0.38 | 17.8 |